Adaptive Robust Trajectory Tracking Control of Fully Actuated Bipedal Robotic Walking

Yan Gu[1] and Chengzhi Yuan[2]

Abstract— **Uncertainties are prevalent in real-world applications of bipedal walking robots, which may deteriorate the robot's locomotion performance and even cause instability. However, designing controllers to address uncertainties for bipedal robotic walking is challenging mainly due to the high complexity of the hybrid walking dynamics under uncertainties. In this paper, an adaptive robust control strategy is proposed by combining control Lyapunov functions and the construction of multiple Lyapunov functions for provably guaranteeing the trajectory tracking performance of bipedal robots in the presence of uncertainties such as modeling errors and disturbances. Simulation results on a three-dimensional bipedal robot with nine revolute joints are conducted to illustrate that the proposed adaptive robust control law can ensure satisfactory tracking performance in the presence of parametric modeling uncertainties and unmodeled nonlinearities.**

I. Introduction

Legged robots can potentially be used to perform locomotion tasks for a wide range of real-world operations such as emergence response, search and rescue, and home assistance. These locomotion tasks can often be translated into tasks of tracking the planned motions such as the planned joint position trajectories. However, enabling legged robots to reliably perform trajectory tracking tasks remains a challenging controller design problem. One of the main causes of the challenge is that uncertainties are pevalent during real-world robot operations. Parametric modeling errors and uncertain disturbances are common examples of these uncertainties. Parametric modeling errors exist when the modeled values of a system parameter (e.g., a robot's link masses) are different from the actual ones, whereas unmodeled uncertainties represent unmodeled disturbances (e.g., a gust of wind) and dynamic behaviors (e.g., unmodeled joint friction). Without properly addressed, these uncertainties can deteriorate a legged robot's stability and tracking performance, which makes it necessary to design locomotion controllers that can mitigation the negative effects of such uncertainties.

To guarantee the stability and tracking performance of continuous systems in the presence of uncertainties, adaptive and robust control strategies have been intensively investigated. Adaptive controllers [1]–[3] have the remarkable advantage in achieving accurate steady-state tracking in the presence of parametric modeling errors. However, it may not be able to guarantee the stability and the transient tracking performance in the presence of unmodeled uncertainties such as disturbances. In contrast, robust control [4], [5] guarantees satisfactory transient performance of tracking in the presence of unmodeled uncertainties, but it cannot guarantee accurate steady-state tracking. To methodologically combine the complementary advantages of adaptive control and robust control for continuous systems, an adaptive robust control approach [6], [7] has been proposed, which resolves the inherent conflict of the two controller design methodologies by adding a known bound to the estimated parameters in the parameter adaptation law. This approach has been used to significantly improve both the transient and the steady-state trajectory tracking performance for various continuous systems in the presence of parametric modeling errors and unmodeled nonlinearities [8], [9]. However, extending this approach to the class of hybrid systems that include legged robots has not been fully explored, which is a complicated challenge due to the high complexity of hybrid and uncertain legged locomotion dynamics.

Bipedal robotic walking is an inherently hybrid dynamical process, which consists of both continuous motions (e.g., foot swinging motions) and discrete behaviors (e.g., foot-landing impacts) [10]. The discrete behaviors are triggered when the system's state satisfies certain conditions (e.g., the swing foot hitting the walking surface), and can cause sudden jumps in a robot's joint velocities. Due to the infinitesimal period of duration, the jumps cannot be directly controlled, thus posing a difficult challenge for tracking controller design.

To explicitly address the state-triggered jumps, controller design for bipeda walking robots have been intensively investigated based on formal stability analysis. The Hybrid Zero Dynamics (HZD) framework [10] is the first control approach that provably stabilizes bipedal walking robots. Its orbitally stabilizing controller can drive a robot's state to converge to the desired orbit in the state space. Recently, the HZD framework has been extended to address uncertainties common in bipedal walking operations. To guarantee the tracking performance of bipedal robots that walking over terrains with uncertain heights, finite state machines have been utilized to guide the switching between multiple controls designed for different terrain heights [11]. Moreover, robust optimal control approaches for bipedal walking have been introduced to deal with modeling uncertainties [12]. The effectiveness of these approaches in handling uncertainties has been experimentally validated on physical bipedal robots. However, orbitally stabilizing controllers cannot gurantee reliable trajectory tracking [13].

[1]Yan Gu is with the Department of Mechanical Engineering, University of Massachusetts Lowell, Lowell, MA 01854, U.S.A. Email: yan_gu@uml.edu.

[2]Chengzhi Yuan is with the Department of Mechanical, Industrial and Systems Engineering, University of Rhode Island, Kingston, RI 02881, U.S.A. Email: cyuan@uri.edu.

Our previous work has introduced a Lyapunov-based trajectory tracking controller design based on the explicit analysis of the Lyapunov fucntion evolution across state-triggered jumps [14]–[16]. However, our previous control approach is synthesized based on input-ouput linearization, which is valid under the assumption that the model is accurately known and no disturbances exist.

The objective of this study is to extend adaptive robust control from continuous systems to hybrid systems with state-triggered jumps that include fully actuated bipedal walking robots for provably guaranteeing the tracking performance under parametric uncertainties and disturbances. There are three main contributions of this study:

(a) To synthesize adaptive robust control laws for hybrid systems with state-triggered jumps by combining control Lyapunov function and the construction of multiple Lyapunov functions.
(b) To explicitly analyze the convergence of parametric estimation and tracking error across state-triggered jumps.
(c) To provide sufficient conditions under which the proposed adaptive robust control will provably guarantee the tracking performance of single-domain fully actuated hybrid systems with state-triggered jumps under parametric uncertainties and disturbances.

This paper is structured as follows. Section II presents the hybrid dynamic model of bipedal walking robots. Section III explains the continuous-phase adaptive robust control law. In Section IV, sufficient closed-loop stability conditions are established, which can be used to guide the specific design of the adaptive robust controller. Simulation results on 3-D bipedal robotic walking are given in Section V.

II. Hybrid Walking Dynamics

This section presents the full-order dynamics of fully-actuated bipedal robotic walking. This model serves as a basis for the proposed adaptive robust controller design.

Bipedal robotic walking is an inherently hybrid dynamical process [10]. The robot's dynamics are described by ordinary differential equations during the continuous phases when the swing foot moves in the air. The robot's joint velocities can experience a suddent jump when the swing foot strikes the group, which are referred to as state-triggered jumps or impulse effects.

A 3-D bipedal robot [17] is shown in Fig. 1. The biped has identical legs and nine revoluate joints. It is assumed that the double-support phase when both legs are in contact with the ground is instantaneous and that the foot landing impact is a contact between rigid bodies. Also, it is assumed that the walking surface is flat and horizontal. Then, a complete walking step consists of a continuous phase and a discrete foot-landing impact .

Let $Q \subset \mathbb{R}^9$ be the configuration space of the robot. Let $U \subset \mathbb{R}^9$ be the set of admissible joint torques. Let $\mathbf{q} = \left[q_1, q_2, q_3, q_4, q_5, q_6, q_7, q_8, q_9\right]^T \in Q$ and $\mathbf{u} = \left[u_1, u_2, u_3, u_4, u_5, u_6, u_7, u_8, u_9\right]^T \in U$ be the vectors of joint positions and torques, respectively. Figure 1 illustrates the definitions of q_i and u_i $(i = 1, 2, \ldots, 9)$. The biped is fully

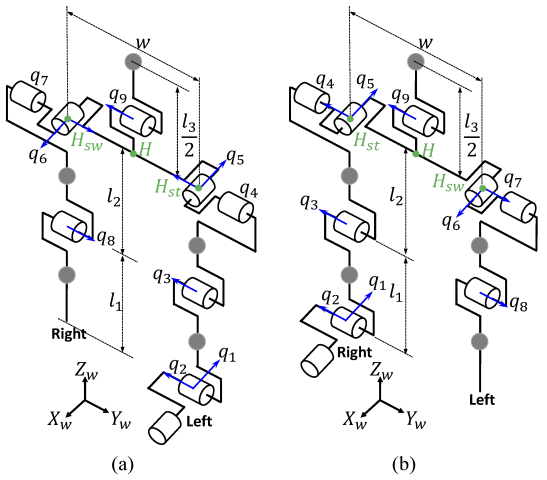

Fig. 1. A 3-D biped with nine revoluate joints. (a): Left leg is in support. (b): Right leg is in support. l_1, l_2, and l_3 are lengths of the lower limb, upper limb, and trunk, respectively. w is the hip width.

actuated because the number of degrees of freedom matches that of the actuators during a continuous phase,

During continuous phases, the full-order dynamic model can be expressed as

$$\mathbf{M}(\mathbf{q}, \boldsymbol{\beta})\ddot{\mathbf{q}} + \mathbf{C}(\mathbf{q}, \dot{\mathbf{q}}, \boldsymbol{\beta})\dot{\mathbf{q}} + \mathbf{G}(\mathbf{q}, \boldsymbol{\beta}) + \tilde{\mathbf{f}}(t, \mathbf{q}, \dot{\mathbf{q}}) = \mathbf{B}_u \mathbf{u}, \quad (1)$$

where $\boldsymbol{\beta} \in \Omega_\beta$ is the vector of model parameters with uncertain values, $\mathbf{M} : Q \times \Omega_\beta \to \mathbb{R}^{9\times 9}$ is the inertia matrix, $\mathbf{C} : TQ \times \Omega_\beta \to \mathbb{R}^{9\times 9}$ is the Coriolis matrix, $\mathbf{G} : Q \times \Omega_\beta \to \mathbb{R}^9$ is the gravitational term, $\tilde{\mathbf{f}} : \mathbb{R}^+ \times TQ \to \Omega_{\tilde{f}}$ is the sum of unmodeled uncertainties such as joint friction, disturbances, and measurement noise, and $\mathbf{B}_u \in \mathbb{R}^{9\times 9}$ is a nonsingular input matrix. TQ is the tangential space of Q. $\Omega_\beta \subset \mathbb{R}^{n_p}$ and $\Omega_{\tilde{f}} \subset \mathbb{R}^9$ are known bounded sets.

The continuous-phase dynamics in Eq. (1) has the following properties [18], [19]:

(P1) The inertia matrix $\mathbf{M}$ is symmetric positive definite, and for any $\mathbf{q} \in Q$ there exist positive numbers k_m and k_M such that

$$k_m \mathbf{I}_{n\times n} \leq \mathbf{M} \leq k_M \mathbf{I}_{n\times n}, \quad (2)$$

where $\mathbf{I}_{n\times n} \in \mathbb{R}^{n\times n}$ is an identity matrix.

(P2) The Coriolis matrix $\mathbf{C}$ can be chosen such that $\mathbf{N} := \dot{\mathbf{M}} - 2\mathbf{C}$ is skew-symmetric.

The vector $\boldsymbol{\beta}$ considered in this study consists of unknown parameters that can be used to linearly parameterize $\mathbf{M}$, $\mathbf{C}$, and $\mathbf{G}$ as:

$$\begin{aligned} &\mathbf{M}(\mathbf{q}, \boldsymbol{\beta})\ddot{\mathbf{q}}_r + \mathbf{C}(\mathbf{q}, \dot{\mathbf{q}}, \boldsymbol{\beta})\dot{\mathbf{q}}_r + \mathbf{G}(\mathbf{q}, \boldsymbol{\beta}) \\ &=: \mathbf{f}_0(\mathbf{q}, \dot{\mathbf{q}}, \dot{\mathbf{q}}_r, \ddot{\mathbf{q}}_r) + \mathbf{Y}(\mathbf{q}, \dot{\mathbf{q}}, \dot{\mathbf{q}}_r, \ddot{\mathbf{q}}_r)\boldsymbol{\beta}, \end{aligned} \quad (3)$$

where $\mathbf{f}_0 \in \mathbb{R}^n$, $\mathbf{Y} \in \mathbb{R}^{n\times n_p}$, and $\mathbf{q}_r \in \mathbb{R}^n$ is any reference vector. An example of $\boldsymbol{\beta}$ is a vector of the robot's link masses.

Given that uncertainties, such as unmodeled joint frictions and unknown link masses, are typically bounded during real-world robot operations [20], it is reasonable to assume the model uncertainties are bounded:

(A1) The true value of $\boldsymbol{\beta}$ is bounded by known vectors, $\boldsymbol{\beta}_{\min}$ and $\boldsymbol{\beta}_{\max}$, as:

$$\boldsymbol{\beta} \in [\boldsymbol{\beta}_{\min}, \boldsymbol{\beta}_{\max}]. \tag{4}$$

(A2) The nonlinear function $\tilde{\mathbf{f}}$ is bounded by a known scalar function $h_f(t, \mathbf{q}, \dot{\mathbf{q}})$ as:

$$\|\tilde{\mathbf{f}}(t, \mathbf{q}, \dot{\mathbf{q}})\| \leq h_f(t, \mathbf{q}, \dot{\mathbf{q}}). \tag{5}$$

An impact occurs when the swing leg strikes the walking surface. Because the swing and the support leg switch roles, their joint positions will experience a sudden jump. Also, the joint velocities will experience a sudden jump due to both the coordinate swap and the rigid-body impact. This state-triggered discrete behavior can be expressed as:

$$\begin{bmatrix} \mathbf{q}^+ \\ \dot{\mathbf{q}}^+ \end{bmatrix} = \boldsymbol{\Delta}(\mathbf{q}^-, \dot{\mathbf{q}}^-, \boldsymbol{\beta}) \tag{6}$$

where $\star^+$ and $\star^-$ represent the values of $\star$ right before or after an impact, respectively. The derivation of $\boldsymbol{\Delta}$ is given in [21].

The occurence of a swing-foot landing is determined by the following switching surface:

$$\begin{aligned} S_q(\mathbf{q}, \dot{\mathbf{q}}, \boldsymbol{\beta}) := \{(\mathbf{q}, \dot{\mathbf{q}}, \boldsymbol{\beta}) \in TQ : & z_{sw}(\mathbf{q}, \boldsymbol{\beta}) = 0, \\ & \dot{z}_{sw}(\mathbf{q}, \dot{\mathbf{q}}, \boldsymbol{\beta}) < 0\}, \end{aligned} \tag{7}$$

where z_{sw} is the swing foot height. Note that the switching surface is not a function of $\boldsymbol{\beta}$ because the swing foot height z_{sw} is not dependent on the robot's masses.

The overall hybrid system dynamics can be expressed as:

$$\begin{cases} \mathbf{M}\ddot{\mathbf{q}} + \mathbf{C}\dot{\mathbf{q}} + \mathbf{G} + \tilde{\mathbf{f}} = \mathbf{B}_u \mathbf{u}, & \text{if } (\mathbf{q}^-, \dot{\mathbf{q}}^-) \notin S_q(\mathbf{q}, \dot{\mathbf{q}}, \boldsymbol{\beta}); \\ \begin{bmatrix} \mathbf{q}^+ \\ \dot{\mathbf{q}}^+ \end{bmatrix} = \boldsymbol{\Delta}, & \text{if } (\mathbf{q}^-, \dot{\mathbf{q}}^-) \in S_q(\mathbf{q}, \dot{\mathbf{q}}, \boldsymbol{\beta}). \end{cases} \tag{8}$$

III. Continuous-Phase Adaptive Robust Control

This section introduces a continuous adaptive robust control approach that mitigates parametric uncertainties and unmodeled nonlinearitie during continuous phases.

The control law is chosen as continuous because only continuous phases can be directly affected by control action. The duration of the state-triggered jump is infinitesimally short, and thus they cannot be directly controlled. Due to the uncontrolled jumps, a continuous control law cannot automatically guarantee the stability and tracking perfrmance of the overall hyrbrid systems ever if it can provably guarantee the stability and trakcing performance for the continuous dynamics. Therefore, in Section IV, we will incorporate the construction of multiple Lyapunov functions into control Lyapunov functions to derive sufficient conditions under which a continuous-phase adaptive robust control law can provably guarantee the stability and tracking performance of the overall hybrid system even in the presence of parametric modeling uncertainties and unmodeled nonlinear uncertianties.

With the model assumptions in Section I, the robot shown in Fig. 1 is fully actuated because it has n revolute joints and n independent actuators. Therefore, n independent variables of interest can be commanded to track n desired trajectories. Let $\mathbf{q}_d(t)$ be the desired trajectories of $\mathbf{q}$. Let $\mathbf{e} := \mathbf{q} - \mathbf{q}_d$ be the joint trajectory tracking errors. The control objective is to design a continuous control law such that the overall hybrid closed-loop system is stable and that the tracking error $\mathbf{e}$ is bounded at the steady state for the hybrid dynamical system with model uncertainties as shown in Eq. (1).

A. Deterministic Robust Control

As shown in Fig. 2, a continuous adaptive robust control law consists of four components [22]. The forward term is used to compensate for the nonlinear dynamics. The linear stabilzing feedback term is used to stabilize the system. The parameter adaptation law is used to estimate the true values of the uncertain model parameters, thus improving the steady-state tracking accuracy. The nonlinear robust feedback term is needed to mitigating the negative effects of uncertain disturbances on the system stability and tracking performances. Without this robust feedback term, a control law consisting of the other three terms may not be able to guarantee stability and transient tracking performance even under small measurement noise and disturbances.

We choose to use sliding mode control (SMC) [22] to form the robust feedback term as previous work [23] has validated its enhanced performance in rejecting uncertainties for legged locomotion.

To guarantee satisfactory tracking performance while the state is reaching or within the sliding mode, a dynamic compensator is introduced: where $\mathbf{A}_c \subset \mathbb{R}^{n_c \times n_c}$, $\mathbf{B}_c \subset \mathbb{R}^{n_c \times n_c}$, $\mathbf{C}_c \subset \mathbb{R}^{n \times n_c}$ and $\mathbf{D}_c \subset \mathbb{R}^{n \times n}$. The matrices are chosen such that ($\mathbf{A}_c$, $\mathbf{B}_c$, $\mathbf{C}_c$, $\mathbf{D}_c$) is controllable and observable.

Introduce a variable $\boldsymbol{\xi}$:

$$\boldsymbol{\xi} = \dot{\mathbf{e}} + \mathbf{y}_c =: \dot{\mathbf{q}} - \dot{\mathbf{q}}_r, \tag{9}$$

where $\dot{\mathbf{q}}_r := \dot{\mathbf{q}}_d - \mathbf{y}_c$. The objective of the sliding mode controller is to ensure that $\boldsymbol{\xi}$ remains zero.

Define $\mathbf{z} := \begin{bmatrix} \mathbf{x}_c \\ \mathbf{e} \end{bmatrix}$. Then,

$$\begin{cases} \dot{\mathbf{z}} = \mathbf{A}_z \mathbf{z} + \mathbf{B}_z \boldsymbol{\xi}; \\ \mathbf{y}_z = \mathbf{C}_z \mathbf{z}, \end{cases} \tag{10}$$

where $\mathbf{A}_z := \begin{bmatrix} \mathbf{A}_c & \mathbf{B}_c \\ -\mathbf{C}_c & -\mathbf{D}_c \end{bmatrix}$, $\mathbf{B}_z := \begin{bmatrix} \mathbf{0} \\ \mathbf{I}_{n \times n} \end{bmatrix}$, and $\mathbf{C}_z := \begin{bmatrix} \mathbf{0} & \mathbf{I}_{n \times n} \end{bmatrix}$.

Therefore, the transfer function matrix from $\boldsymbol{\xi}$ to $\mathbf{e}$ is

$$\mathbf{G}_{\xi}^{-1}(s) := (s\mathbf{I}_{n \times n} + \mathbf{G}_c(s))^{-1},$$

where $\mathbf{G}_c(s) := \mathbf{C}_c(s\mathbf{I}_{n_c} - \mathbf{A}_c)^{-1}\mathbf{B}_c + \mathbf{D}_c$. By carefully assigning the poles of $\mathbf{G}_{\xi}$, the desired response during the transient reaching phase can be achieved.

The robust feedback term can be expressed as:

$$\mathbf{u}_r = \hbar(-h_s \frac{\boldsymbol{\xi}}{\|\boldsymbol{\xi}\|}), \tag{11}$$

where $\hbar(-h_s \frac{\boldsymbol{\xi}}{\|\boldsymbol{\xi}\|})$ is a continuous approximation of the ideal

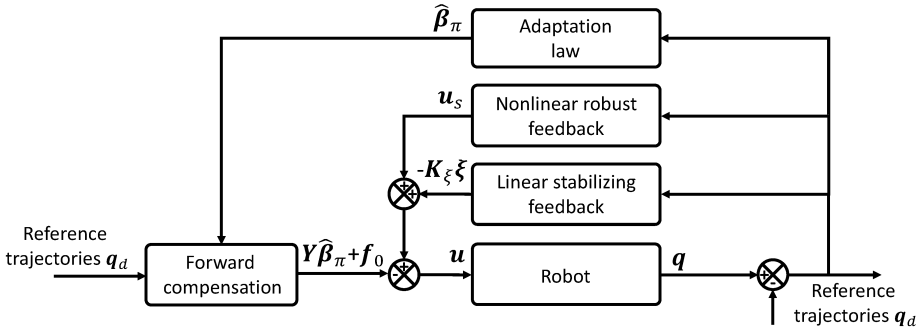

Fig. 2. Block diagram of a continuous adaptive robust control law.

sliding mode control, $h_s\frac{\boldsymbol{\xi}}{\|\boldsymbol{\xi}\|}$, with a known approximation error $\varepsilon(t)$.

Various forms of $\hbar$ could be used as continuous approximations of the ideal sling mode control. Here, we choose to adopt the following definition of $\hbar$ among others [1], [24] because it is relatively easy to implement thanks to its simple expression:

$$\hbar(-h_s\frac{\boldsymbol{\xi}}{\|\boldsymbol{\xi}\|})=\begin{cases}-\mathbf{K}_s\boldsymbol{\xi} & \text{if}\|\boldsymbol{\xi}\|\le\phi_h\\ -(1-c_1)\mathbf{K}_s\boldsymbol{\xi}-c_1h_s\frac{\boldsymbol{\xi}}{\|\boldsymbol{\xi}\|} & \text{if}\phi_h\le\|\boldsymbol{\xi}\|\le(1+\varepsilon_2)\phi_h\\ -h_s\frac{\boldsymbol{\xi}}{\|\boldsymbol{\xi}\|} & \text{if}\|\boldsymbol{\xi}\|\ge(1+\varepsilon_2)\phi_h\end{cases} \tag{12}$$

where $\mathbf{K}_s\in\mathbb{R}^{9\times9}$ is any symmetric positive definite matrix, and ε_1 and ε_2 are any positive scalars. $\phi_h:=\frac{\phi}{h_s(t,\mathbf{q},\dot{\mathbf{q}},\dot{\mathbf{q}}_r,\ddot{\mathbf{q}}_r)+\varepsilon_1}$, where $\phi(t)$ is any positive scalar function on $t>0$. $c_1=\frac{\|\boldsymbol{\xi}\|-\phi_h}{\varepsilon_2\phi_h}$. With this choice of $\hbar$, the approximation error ε becomes $\varepsilon(t)=(1+\varepsilon_2)\phi_h(t)$.

Since the initial condition of the dynamic compensator during a walking step can be arbitrarily designed, we can choose the initial value of $\mathbf{z}$ such that $\boldsymbol{\xi}$ is reset to zero at the initial moment of a walking step. Let T_k be the initial moment of the k^{th} walking step ($k\in\{1,2,...\}$). Then, to ensure $\boldsymbol{\xi}(T_k^+)=\mathbf{0}$, $\mathbf{z}(T_k^+)$ is chosen as

$$\mathbf{C}_c\mathbf{z}(T_k^+)=-\dot{\mathbf{e}}(T_k^+)-\mathbf{D}_c\mathbf{e}(T_k^+). \tag{13}$$

B. Parameter Adaptation Law

The parameter adaption law estimates the unknown model parameters $\boldsymbol{\beta}$. The estimated model parameters are then used to form a feedforward term that compensates for the nonlinear dynamics. The main advantage of using parameter adaptation is that: it reduces the modeling error and thus improves the steady-state tracking accuracy without replying on high-gain feedback control.

Let $\hat{\boldsymbol{\beta}}\in\Omega_\beta$ be the estimated value of $\boldsymbol{\beta}$. The parameter adaptation law is defined as:

$$\dot{\hat{\boldsymbol{\beta}}}=-\boldsymbol{\Gamma}\boldsymbol{\tau}, \tag{14}$$

where the adaptation function $\boldsymbol{\tau}$ is

$$\boldsymbol{\tau}=\mathbf{Y}^T(\mathbf{q},\dot{\mathbf{q}},\dot{\mathbf{q}}_r,\ddot{\mathbf{q}}_r)\boldsymbol{\xi}. \tag{15}$$

The parameter estimation law in Eq. (14) can lead to an unbounded parameter estimation error in the presence of unmodeled uncertainty $\tilde{\mathbf{f}}$. However, boundedness of the parameter estimation error is necessary as the robust feedback term introduced in Section III-A requires the knowledge of the bound of the parameter estimation error. To resolve this conflict, the key is to modify the parameter estimation $\hat{\boldsymbol{\beta}}$ into a bounded vector.

Various modifications of the parameter estimation $\hat{\boldsymbol{\beta}}$ have been introduced [22]. We choose to adopt a smooth projection so that the convergence of $\hat{\boldsymbol{\beta}}$ can be explicitly analyzed based on Lyapunov function theory in Section V.

Let $\boldsymbol{\varepsilon}_\beta\in\mathbb{R}^{n_p}$ be a known vector of small positive numbers. Let $\boldsymbol{\pi}(\hat{\boldsymbol{\beta}})$ be a smooth projection of $\hat{\boldsymbol{\beta}}$ that has bounded, sufficiently smooth derivatives and satisfies the following conditions:

(C3) $\boldsymbol{\pi}(\hat{\boldsymbol{\beta}})=\hat{\boldsymbol{\beta}}$ if $\hat{\boldsymbol{\beta}}\in\Omega_\beta$.

(C4) $\boldsymbol{\pi}(\hat{\boldsymbol{\beta}})\in\Omega_{\hat{\beta}}:=[\boldsymbol{\beta}_{\min}-\boldsymbol{\varepsilon}_\beta\quad\boldsymbol{\beta}_{\max}+\boldsymbol{\varepsilon}_\beta]$ if $\hat{\boldsymbol{\beta}}\in\mathbb{R}^{n_p}$.

For notational simplicity, define $\hat{\boldsymbol{\beta}}_\pi:=\boldsymbol{\pi}(\hat{\boldsymbol{\beta}})$. Let $\tilde{\boldsymbol{\beta}}_\pi$ be the parameter estimation error, $\tilde{\boldsymbol{\beta}}_\pi:=\hat{\boldsymbol{\beta}}_\pi-\boldsymbol{\beta}$.

From the assumption (A1), the following inequality holds:

$$\|\mathbf{Y}(\mathbf{q},\dot{\mathbf{q}},\dot{\mathbf{q}}_r,\ddot{\mathbf{q}}_r)\tilde{\boldsymbol{\beta}}_\pi\|\le h_\beta(\mathbf{q},\dot{\mathbf{q}},\dot{\mathbf{q}}_r,\ddot{\mathbf{q}}_r), \tag{16}$$

where the bound can be chosen as

$$h_\beta:=\|\mathbf{Y}(\mathbf{q},\dot{\mathbf{q}},\dot{\mathbf{q}}_r,\ddot{\mathbf{q}}_r)\|\beta_M:=\|\mathbf{Y}(\mathbf{q},\dot{\mathbf{q}},\dot{\mathbf{q}}_r,\ddot{\mathbf{q}}_r)\|\|\boldsymbol{\beta}_{\max}-\boldsymbol{\beta}_{\min}+\boldsymbol{\varepsilon}_\beta\|. \tag{17}$$

C. Overall Control Law

With the robust feedback and the parameter adaptation law designed, the overall continuous ARC can be expressed as:

$$\mathbf{u}=\mathbf{B}_u^{-1}(\mathbf{u}_r+\mathbf{f}_0(\mathbf{q},\dot{\mathbf{q}},\dot{\mathbf{q}}_r,\ddot{\mathbf{q}}_r)+\mathbf{Y}(\mathbf{q},\dot{\mathbf{q}},\dot{\mathbf{q}}_r,\ddot{\mathbf{q}}_r)\hat{\boldsymbol{\beta}}_\pi-\mathbf{K}_\xi\boldsymbol{\xi}), \tag{18}$$

where $\mathbf{K}_\xi\in\mathbb{R}^{n\times n}$ is any symmetric positive definite matrix, the robust feedback term $\mathbf{u}_r$ is given in Eq. (11), and the adaptation law for $\hat{\beta}$ is given in Eq. (14).

IV. Closed-loop Stability Analysis

This section analyzes the stability of the uncertain hybrid systems with state-triggered jumps in Eq. (8) under the proposed continuous ARC. The outcome of the analysis is a set of sufficient conditions that can be used to guide the

selection and tuning of control gains for guaranteeing the closed-loop stability and tracking performance.

The key in the proposed stability analysis is to explicitly analyze the effects of state-triggered jumps on the system stability and tracking performance. Such an explicit analysis is necessary because the jumps cannot be directly controlled due to their infinitesimally short period of duration. Yet, the analysis is intricate for two main reasons: a) the occurrence timing of these state-triggered jumps is an implicit function of system state and b) uncertainties affect the dynamics of the state-triggered jumps.

Let the system state be

$$\mathbf{x} := \begin{bmatrix} \mathbf{z} \\ \boldsymbol{\xi} \end{bmatrix}$$

with $\|\mathbf{x}\| := \sqrt{\|\mathbf{z}\|^2 + \|\boldsymbol{\xi}\|^2}$.

The closed-loop hybrid system under the continuous ARC can be expressed as:

$$\begin{cases} \begin{cases} \mathbf{M}\dot{\boldsymbol{\xi}} + (\mathbf{C}+\mathbf{K}_\xi)\boldsymbol{\xi} = \hbar(-h_s \frac{\boldsymbol{\xi}}{\|\boldsymbol{\xi}\|}) + \mathbf{Y}\tilde{\boldsymbol{\beta}}_\pi - \tilde{\mathbf{f}} \\ \dot{\mathbf{z}} = \mathbf{A}_z\mathbf{z} + \mathbf{B}_z\boldsymbol{\xi} \\ \dot{\tilde{\boldsymbol{\beta}}} = -\boldsymbol{\Gamma}\boldsymbol{\tau} \end{cases} & \text{if } (t,\mathbf{x}^-) \notin S_x; \\ \begin{bmatrix} \boldsymbol{\xi}^+ \\ \mathbf{z}^+ \\ \tilde{\boldsymbol{\beta}}^+ \end{bmatrix} = \begin{bmatrix} \mathbf{0} \\ \boldsymbol{\Delta}_z \\ \tilde{\boldsymbol{\beta}}^- \end{bmatrix} & \text{if } (t,\mathbf{x}^-) \in S_x, \end{cases} \tag{19}$$

where $\tilde{\boldsymbol{\beta}}_\pi := \hat{\boldsymbol{\beta}}_\pi - \boldsymbol{\beta}$. The expression of $\boldsymbol{\Delta}_z(t,\mathbf{z}^-,\boldsymbol{\xi}^-,\boldsymbol{\beta})$ can be obtained from Eqs. (6), (**??**) and (**??**). The expression of S_x can be obtained from Eqs. (7) and (**??**). Note that $\boldsymbol{\Delta}_z$ is explicitly time-dependent because the reference trajectory $\mathbf{q}_d$ is explicitly time-dependent.

Theorem 1: The proposed continuous-phase control law in Eq. (18) locally stabilizes the hybrid system in Eq. (19) if the control gains are chosen such that

(C5) the matrix $\mathbf{A}_z$ is Hurwitz and
(C6) the continuous-phase convergence rate of $\mathbf{x}$ is sufficiently fast.

Proof: Let $V_\xi(\boldsymbol{\xi})$ and $V_z(\mathbf{z})$ be the control Lyapunov function candidates associated with $\boldsymbol{\xi}$ and $\mathbf{z}$, respectively:

$$V_\xi = \frac{1}{2}\boldsymbol{\xi}^T\mathbf{M}\boldsymbol{\xi} \text{ and } V_z = \mathbf{z}^T\mathbf{P}_z\mathbf{z}. \tag{20}$$

By the condition (C5), the matrix $\mathbf{A}_z$ is Hurwitz. Thus, the matrix $\mathbf{P}_z \in \mathbb{R}^{n_c \times n_c}$ can be obtained by solving the following Lyapunov equation [13]:

$$\mathbf{A}_z^T\mathbf{P}_z + \mathbf{P}_z\mathbf{A}_z = -\mathbf{Q}_z, \tag{21}$$

where $\mathbf{Q}_z \in \mathbb{R}^{n_c \times n_c}$ is any symmetric positive definite matrix.

The total control Lyapunov function is defined as:

$$V_t(\mathbf{x}) = V_\xi(\boldsymbol{\xi}) + V_z(\mathbf{z}). \tag{22}$$

To derive the stability conditions, we incorporate the construction of multiple Lyapunov functions into the control Lyapunov functions. According to the stability theory based on the construction of multiple Lyapunov functions [25], a hybrid system is stable if the Lyapunov function decreases during continuous phases and if the values of the Lyapunov function right after each switching event form a strictly decreasing sequence.

Following these criteria, we first derive sufficient stability conditions for continuous phases. Let T_k ($k \in \{1,2,...\}$) be the initial moment of the k^{th} walking step. Define

$$k_1 := \lambda_{\min}(\mathbf{P}_z),\ k_2 := \lambda_{\max}(\mathbf{P}_z),\ \text{and } k_3 := \frac{\lambda_{\min}(\mathbf{Q}_z)}{k_2}, \tag{23}$$

with $\lambda_{\min}(\star)$ and $\lambda_{\min}(\star)$ being the largest and the smallest eigenvalues of $\star$, respectively. From (24), it is guaranteed that for any $\mathbf{z}(0) \in \mathbb{R}^{n_c+n}$

$$k_1\|\mathbf{z}\|^2 \le V_z \le k_2\|\mathbf{z}\|^2 \tag{24}$$

and

$$\dot{V}_z \le -k_3 V_z \tag{25}$$

during the continuous phase of the k^{th} walking step (i.e., $t \in (T_k, T_{k+1}]$).

From Eqs. (2) and (20), there exists a positive number r_ξ such that

$$\frac{1}{2}k_m\|\boldsymbol{\xi}\|^2 \le V_\xi \le \frac{1}{2}k_M\|\boldsymbol{\xi}\|^2 \tag{26}$$

holds for all $\boldsymbol{\xi}(0) \in \{\boldsymbol{\xi} : \|\boldsymbol{\xi}\| \le r_\xi\}$.

From the property (P2), we know that $\dot{\mathbf{M}} - 2\mathbf{C}$ is skew symmetric. Thus,

$$\frac{1}{2}\boldsymbol{\xi}^T\dot{\mathbf{M}}\boldsymbol{\xi} = \boldsymbol{\xi}^T\mathbf{C}\boldsymbol{\xi}. \tag{27}$$

From Eqs. (19), (22), and (27),

$$\begin{aligned} \dot{V}_\xi &= \boldsymbol{\xi}^T\mathbf{M}\dot{\boldsymbol{\xi}} + \frac{1}{2}\boldsymbol{\xi}^T\dot{\mathbf{M}}\boldsymbol{\xi} \\ &= \boldsymbol{\xi}^T(\mathbf{M}\dot{\boldsymbol{\xi}} + \mathbf{C}\boldsymbol{\xi}) \\ &= \boldsymbol{\xi}^T(\mathbf{Y}\tilde{\boldsymbol{\beta}}_\pi - \tilde{\mathbf{f}} - \mathbf{K}_\xi\boldsymbol{\xi} + \hbar(-h_s\tfrac{\boldsymbol{\xi}}{\|\boldsymbol{\xi}\|})) \\ &\le \|\boldsymbol{\xi}\|(\|\mathbf{Y}\tilde{\boldsymbol{\beta}}_\pi\| + \|\tilde{\mathbf{f}}\|) - \boldsymbol{\xi}^T\mathbf{K}_\xi\boldsymbol{\xi} + \boldsymbol{\xi}^T\hbar(-h_s\tfrac{\boldsymbol{\xi}}{\|\boldsymbol{\xi}\|})). \end{aligned} \tag{28}$$

Then, from the condition (C2) and Eqs. (5), (**??**), and (16), we have

$$\dot{V}_\xi \le -\boldsymbol{\xi}^T\mathbf{K}_\xi\boldsymbol{\xi} + \varepsilon(t) \le -\lambda_\xi V_\xi + \varepsilon(t), \tag{29}$$

where

$$\lambda_\xi := \frac{2\lambda_{\min}(\mathbf{K}_\xi)}{k_M}. \tag{30}$$

Therefore, for all $\mathbf{x}(0) \in B_{r_\xi}(\mathbf{0}) := \{\mathbf{x} : \|\mathbf{x}\| \le r_\xi\}$, the total control Lyapunov function V_t satisfies

$$k_{t1}\|\mathbf{x}\|^2 \le V_t(\mathbf{x}) \le k_{t2}\|\mathbf{x}\|^2 \tag{31}$$

and

$$\dot{V}_t \le -k_{t3}V_t + \varepsilon(t) \tag{32}$$

within the continuous phase of the k^{th} walking step, where

$$\begin{aligned} k_{t1} := \min(k_1, \frac{k_m}{2}),\ k_{t2} := \max(k_2, \frac{k_M}{2}), \\ \text{and } k_{t3} := \min(k_3, \lambda_\xi). \end{aligned} \tag{33}$$

Second, we analyze the evolution of V_t across the uncontrolled state-triggered jumps. Because $\boldsymbol{\xi}$ is reset to zero at

the beginning of each walking step, V_ξ is accordingly also reset to zero. Thus, we focus on analyzing the evolution of V_z across the jump $\boldsymbol{\Delta}_z$.

In the following analysis, $\star(T_k^-)$ and $\star(T_k^+)$ are denoted as $\star|_k^-$ and $\star|_k^+$, respectively, for notational simplicity.

The norm of $\mathbf{z}$ after an impact at T_{k+1}^- can be estimated as:

$$\begin{aligned}\|\mathbf{z}|_{k+1}^+\| =&\|\boldsymbol{\Delta}_z(T_{k+1},\mathbf{x}|_{k+1}^-,\boldsymbol{\beta})\|\\ \leq& \|\boldsymbol{\Delta}_z(T_{k+1},\mathbf{x}|_{k+1}^-,\boldsymbol{\beta})-\boldsymbol{\Delta}_z(\tau_{k+1},\mathbf{x}|_{k+1}^-,\boldsymbol{\beta})\|\\ &+\|\boldsymbol{\Delta}_z(\tau_{k+1},\mathbf{x}|_{k+1}^-,\boldsymbol{\beta})-\boldsymbol{\Delta}_z(\tau_{k+1},\mathbf{0},\boldsymbol{\beta})\|\\ &+\|\boldsymbol{\Delta}_z(\tau_{k+1},\mathbf{0},\boldsymbol{\beta})-\boldsymbol{\Delta}_z(\tau_{k+1},\mathbf{0},\hat{\boldsymbol{\beta}}_\pi)\|\\ &+\|\boldsymbol{\Delta}_z(\tau_{k+1},\mathbf{0},\hat{\boldsymbol{\beta}}_\pi)\|,\end{aligned} \tag{34}$$

where τ_{k+1} ($k\in\{1,2,...\}$) is the planned initial moment of the $(k+1)^{th}$ walking step.

Suppose that the reference trajectories are planned to respect the estimated reset map, i.e.,

$$\boldsymbol{\Delta}_z(\tau_{k+1},\mathbf{0},\hat{\boldsymbol{\beta}}_\pi)=\mathbf{0},$$

which can be guaranteed through the planning of the reference trajectory [10].

Note that the reset map $\boldsymbol{\Delta}_z$ is continuously differentiable in t, $\mathbf{x}$, and $\boldsymbol{\beta}$. Thus, there exists a positive number r_1 such that $\boldsymbol{\Delta}_z$ is Lipschitz continuous in these variables for any $\mathbf{x}(0)\in B_{r_1}(\mathbf{0})$. Accordingly, the approximation of $\|\mathbf{z}|_{k+1}^+\|$ becomes:

$$\begin{aligned}\|\mathbf{z}|_{k+1}^+\| =&\|\boldsymbol{\Delta}_z(T_{k+1},\mathbf{x}|_{k+1}^-,\boldsymbol{\beta})\|\\ \leq& L_T|T_{k+1}-\tau_{k+1}|+L_x\|\mathbf{x}|_{k+1}^-\|+L_\beta\|\boldsymbol{\beta}-\hat{\boldsymbol{\beta}}_\pi\|,\end{aligned} \tag{35}$$

where the positive numbers L_T, L_x, and L_β are Lipschitz constants.

From Eq. (17),

$$\|\boldsymbol{\beta}-\hat{\boldsymbol{\beta}}_\pi\|=\|\tilde{\boldsymbol{\beta}}_\pi\|\leq\beta_M. \tag{36}$$

Since $\hbar(-h_s\frac{\boldsymbol{\xi}}{\|\boldsymbol{\xi}\|})$ and $\mathbf{Y}\hat{\boldsymbol{\beta}}_\pi$ are continuous in t, $\mathbf{x}$, and $\hat{\boldsymbol{\beta}}_\pi$, there exist positive numbers k_T and r_2 such that

$$|T_{k+1}-\tau_{k+1}|\leq k_T\|\mathbf{x}|_{k+1}^-\| \tag{37}$$

for any $\mathbf{x}(0)\in B_{r_2}(\mathbf{0})$ [26].

Therefore, from Eqs. (35)-(37),

$$\|\mathbf{z}|_{k+1}^+\|\leq(L_Tk_T+L_x)\|\mathbf{x}|_{k+1}^-\|+L_\beta\beta_M. \tag{38}$$

Accordingly,

$$\|\mathbf{z}|_{k+1}^+\|^2\leq L_{\Delta x}\|\mathbf{x}|_{k+1}^-\|^2+2L_\beta^2\beta_M^2, \tag{39}$$

where $L_{\Delta x}:=2(L_Tk_T+L_x)^2$.

Because $\boldsymbol{\xi}|_{k+1}^+=\mathbf{0}$, we have $V_\xi|_{k+1}^+=0$. Therefore, from Eqs. (22), (24), (26), and (39),

$$V_t|_{k+1}^+\leq\frac{k_{t2}L_{\Delta x}}{k_{t1}}V_t|_{k+1}^-+2k_{t2}L_\beta^2\beta_M^2. \tag{40}$$

From Eq. (32),

$$V_t|_{k+1}^-\leq\int_{T_k}^{T_{k+1}}e^{-k_{t3}(T_{k+1}-\nu)}\varepsilon(\nu)d\nu+e^{-k_{t3}(T_{k+1}-T_k)}V_t|_k^+. \tag{41}$$

Therefore,

$$\begin{aligned}V_t|_{k+1}^+\leq&\frac{k_{t2}L_{\Delta x}}{k_{t1}}e^{-k_{t3}(T_{k+1}-T_k)}V_t|_k^+\\ &+\frac{k_{t2}L_{\Delta x}}{k_{t1}}\int_{T_k}^{T_{k+1}}e^{-k_{t3}(T_{k+1}-\nu)}\varepsilon(\nu)d\nu\\ &+2k_{t2}L_\beta^2\beta_M^2.\end{aligned} \tag{42}$$

Let $\varepsilon_{\max}$ be the bound of $\varepsilon(t)$. Then,

$$\varepsilon(t)\leq\varepsilon_{\max} \tag{43}$$

holds for all t. Thus,

$$\int_{T_k}^{T_{k+1}}e^{-k_{t3}(T_{k+1}-\nu)}\varepsilon(\nu)d\nu\leq\frac{\varepsilon_{\max}}{k_{t3}}(1-e^{-k_{t3}\Delta T_k}), \tag{44}$$

where $\Delta T_k:=T_{k+1}-T_k$ is the duration of the k^{th} step.

Combining Eqs. (42)-(44) yields

$$V_t|_{k+1}^+\leq\delta_kV_t|_k^++b_k, \tag{45}$$

where

$$\delta_k:=\frac{k_{t2}L_{\Delta x}}{k_{t1}}e^{-k_{t3}\Delta T_k}$$

and

$$b_k:=2k_{t2}L_\beta^2\beta_M^2+\frac{k_{t2}L_{\Delta x}\varepsilon_{max}}{k_{t1}k_{t3}}(1-e^{-k_{t3}\Delta T_k}).$$

From Eq. (37), we know that ΔT_k is bounded. Hence, there exist positive numbers $\Delta T_{\min}$ and $\Delta T_{\max}$ such that $\Delta T_{\min}\leq\Delta T_k\leq\Delta T_{\max}$ holds for all $k\in\{1,2,...\}$. Then,

$$\delta_k\leq\delta_{\max}:=\frac{k_{t2}L_{\Delta x}}{k_{t1}}e^{-k_{t3}\Delta T_{\min}} \tag{46}$$

and

$$b_k\leq b_{\max}:=2k_{t2}L_\beta^2\beta_M^2+\frac{k_{t2}L_{\Delta x}\varepsilon_{\max}}{k_{t1}k_{t3}}(1-e^{-k_{t3}\Delta T_{\max}}). \tag{47}$$

By the condition (C6), the continuous-phase convergence rate k_{t3} is sufficiently fast and thus can be chosen to satisfy

$$k_{t3}>\frac{1}{\Delta T_{\min}}ln(\frac{k_{t2}L_{\Delta x}}{k_{t1}}). \tag{48}$$

Then, from Eq. (46), we have

$$\delta_{\max}<1. \tag{49}$$

Therefore, for any $k\in\{1,2,...\}$, we have

$$V_t|_{k+1}^+\leq\delta_{\max}^{k+1}V_t|_0^++\frac{1-\delta_{\max}^{k+1}}{1-\delta_{\max}}b_{\max} \tag{50}$$

for any $\mathbf{x}(0)\in B_r(\mathbf{0})$ where $r=\min(r_\xi,r_1,r_2)$. Accordingly, when $k\to\infty$, i.e., when $t\to\infty$, we have

$$V_t|_\infty^+\to\frac{b_{\max}}{1-\delta_{\max}}, \tag{51}$$

which indicates that $\|\mathbf{x}\|$ exponentially converges to a final, bounded value for the overall hybrid dynamical process.

V. Simulations

This section presents simulation results of 3-D bipedal robotic walking for validating the effectiveness of the proposed controller design method in guaranteeing stability and tracking performance under parametric uncertainties and unmodeled uncertainties.

A. Simulation Setup

As stated in Section III, the control objective are to stabilize the uncertain hybrid system with state-triggered jumps in Eq. (8) and to drive the actual joint trajectory $\mathbf{q}$ to the desired one $\mathbf{q}_d(t)$ with a bounded final tracking error.

To achieve the control objective, it is necessary to properly tune the controller parameters for stabilizing the closed-loop system and for achieving a reliable tracking performance. These controller parameters include: a) the gain of the linear stabilizing feedback term, $\mathbf{K}_\xi$; b) the gain of the parameter adaptation law, $\mathbf{\Gamma}$; c) and the parameters of the robust controller, including the matrices of the dynamic compensator (i.e., $\mathbf{A}_c$, $\mathbf{B}_c$, $\mathbf{C}_c$, and $\mathbf{D}_c$) and the parameters of the SMC (i.e., $\mathbf{K}_s$, ϕ, ε_1, and ε_2).

The general rules for tuning these controller parameters include: a) a larger $\mathbf{K}_\xi$ generally increases the rate of convergence of the tracking error; b) a larger $\mathbf{\Gamma}$ can result in faster convergence of the estimated parameters to their true values; c) faster poles of the dynamic compensator (i.e., the poles of $(s\mathbf{I}_{n\times n}+\mathbf{G}_c(s))^{-1}$) can lead to faster convergence of the tracking error; d) a smaller ϕ, a lager ε_1, or a smaller ε_2 can all expand the range of states that the ideal SMC (i.e., $-h_s\frac{\boldsymbol{\xi}}{\|\boldsymbol{\xi}\|}$) acts on.

The parameters of the controllers are chosen as follows. The control law is formed as in Section V. The dynamic compensator is set as: $\mathbf{A}_c=\mathbf{0}_{9\times 9}$, $\mathbf{B}_c=100\mathbf{I}_{9\times 9}$, $\mathbf{C}_c=\mathbf{I}_{9\times 9}$, and $\mathbf{D}_c=2\omega\mathbf{I}_{9\times 9}$ ($\omega_c=10$), which render the corner frequency of the sliding mode as $\omega_c=10$. The parameters of the SMC are chosen as: $\phi=30$, $\varepsilon_1=1$, and $\varepsilon_2=0.5$. The adaptation gain is chosen as $\mathbf{\Gamma}=40\mathbf{I}_{3\times 3}$. The linear stabilizing feedback gains for $\boldsymbol{\xi}$ are chosen as $\mathbf{K}_\xi=40\mathbf{I}_{9\times 9}$ and $\mathbf{K}_s=20\mathbf{I}_{9\times 9}$. These gains produce an overall feedback gain for $\boldsymbol{\xi}$ as $\mathbf{K}_\xi+\mathbf{K}_s=60\mathbf{I}_{9\times 9}$.

The following settings are used in the simulations:

(a) the maximum norm of the unmodeled uncertainty is 30, i.e., $h_f=30$;

(b) the initial position and velocity tracking errors of each joint are 0.2 rad (about 11°) and 0.3 rad/s (about 17°/s), respectively;

(c) the unknown parameters are the robot's link masses, i.e., $\boldsymbol{\beta}=[m_1\ m_2\ m_T]^T=[0.4\ 0.8\ 4.8]^T$;

(d) the lower and the upper bounds of the parameter estimation are set as $\boldsymbol{\beta}_{\min}=[-1.1\ \ -0.4\ \ -1.2]^T$ kg and $\boldsymbol{\beta}_{\max}=[3.4\ 2.3\ 16.8]$ kg, respectively. This setting allows us to assess the performance of ARC under relatively large bounds of parameter estimation;

(e) the initial parameter estimation is $\hat{\boldsymbol{\beta}}_0=\hat{\boldsymbol{\beta}}_{\pi 0}=[2.7\ 2.1\ 10.8]^T$ kg, corresponding to an initial estimation error of $\tilde{\boldsymbol{\beta}}_0=\tilde{\boldsymbol{\beta}}_{\pi 0}=[2.3\ 1.3\ 6]^T$ kg.

B. Simulation Results

The simulation results are shown in Figs. 3 and 4. The control performance is analyzed as follows:

Final tracking error and convergence rate: To evaluate the transient tracking performance and the final tracking accuracy of the controllers, we assess the rate of the actual trajectory converges to the desired trajectory as well as the magnitude of the tracking error close to the steady state. Thanks to the nonlinear robust feedback term, the RC and As shown in the figures, the ARC is able to achieve good final tracking accuracy and relatively fast transient convergence.

Control effort demanded: Simulations results show that ARC demands a reasonable level of control effort for stabilization even under uncertainties, which illustrates the advantage of enforcing a finite bound to the parameter estimation, which is missing in the design of AC.

Control chattering: Due to the use of aggressive nonlinear robust feedback, i.e., the modified SMC, the ARC may be subject to certain amount of control chattering, especially at the initial period of each walking step, as shown in the figures. During these initial periods, the idea SMC is activated to reject the tracking error divergence caused by the uncontrolled state-triggered jumps upon foot-landing events. However, the chattering effect is not significant thanks to the incorporation of parameter estimation.

Parameter estimation boundedness: Simulation results show that the ARC achieves a small estimation error without causing an overly large joint torque thanks to the smooth projection of parameter estimation, as shown in Fig. 3.

Robustness: To evaluate the robustness of the RC and the ARC, the nonlinear function $\tilde{\mathbf{f}}$ is modified to include an additional term, $10\cdot(-1)^{\frac{t}{0.2}}$. Simulation results are shown in Fig. 4. As shown in the figures, the tracking performance is close to the cases where the additional nonlinear function term is absent (i.e., Fig. 3), which validates the robustness of the ARC in rejecting unmodeled uncertainties.

VI. Conclusions

An adaptive robust control law has been proposed to achieve accurate joint position tracking in the presence of unknown modeling errors and disturbances. The control law was proposed based on the full-order nonlinear, hybrid dynamcis of bipedal robotic walking with full actuation. Simulated walking experiments showed that the proposed ARC can effectively guarantee the tracking performance under model parametric errors and unmodeled uncertainties.

References

[1] J.-J. E. Slotine, W. Li *et al.*, *Applied nonlinear control*. Prentice hall Englewood Cliffs, NJ, 1991, vol. 199, no. 1.

[2] M. Krstic, P. V. Kokotovic, and I. Kanellakopoulos, *Nonlinear and adaptive control design*. John Wiley & Sons, Inc., 1995.

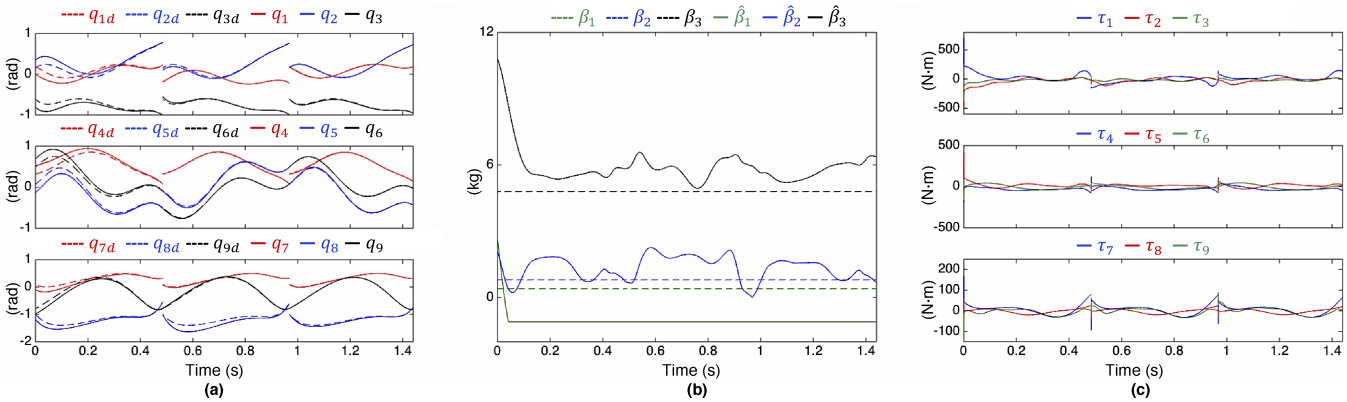

Fig. 3. Tracking results of Adaptive Robust Control (Case 4) during three simulated walking steps. a) Joint position tracking. b) Parameter estimation. c) Joint torque profiles.

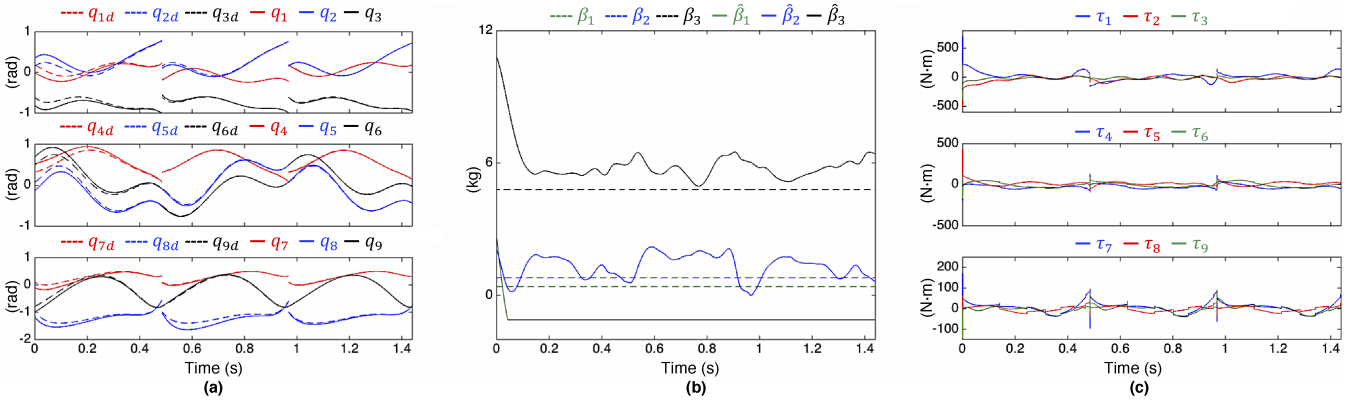

Fig. 4. Tracking results of Adaptive Robust Control in the presence of unmodeled nonlinearities different from Case 4. a) Joint position tracking. b) Parameter estimation. c) Joint torque profiles.

[3] S. Sastry and M. Bodson, *Adaptive control: stability, convergence and robustness*. Courier Corporation, 2011.

[4] K. Zhou and J. C. Doyle, *Essentials of robust control*. Prentice hall Upper Saddle River, NJ, 1998, vol. 104.

[5] S. Skogestad and I. Postlethwaite, *Multivariable feedback control: analysis and design*. Wiley New York, 2007, vol. 2.

[6] B. Yao and M. Tomizuka, "Adaptive robust control of siso nonlinear systems in a semi-strict feedback form," *Automatica*, vol. 33, no. 5, pp. 893–900, 1997.

[7] ——, "Adaptive robust control of mimo nonlinear systems in semi-strict feedback forms," *Automatica*, vol. 37, no. 9, pp. 1305–1321, 2001.

[8] C. Hu, B. Yao, and Q. Wang, "Coordinated adaptive robust contouring controller design for an industrial biaxial precision gantry," *IEEE/ASME Transactions on Mechatronics*, vol. 15, no. 5, pp. 728–735, 2009.

[9] B. Yao, C. Hu, and Q. Wang, "An orthogonal global task coordinate frame for contouring control of biaxial systems," *IEEE/ASME Transactions on Mechatronics*, vol. 17, no. 4, pp. 622–634, 2011.

[10] J. Grizzle, G. Abba, and P. Plestan, "Asymptotically stable walking for biped robots: Analysis via systems with impulse effects," *IEEE Trans. Autom. Contr.*, vol. 46, no. 1, pp. 51–64, 2001.

[11] H.-W. Park, A. Ramezani, and J. W. Grizzle, "A finite-state machine for accommodating unexpected large ground-height variations in bipedal robot walking," *IEEE Trans. Robot.*, vol. 29, no. 2, pp. 331–345, 2013.

[12] Q. Nguyen and K. Sreenath, "Optimal robust control for bipedal robots through control lyapunov function based quadratic programs." in *Robotics: Science and Systems*. Rome, Italy, 2015.

[13] H. K. Khalil, *Nonlinear control*. Prentice Hall, 1996.

[14] Y. Gu, B. Yao, and C. S. G. Lee, "Bipedal gait recharacterization and walking encoding generalization for stable dynamic walking," in *Proc. IEEE Int. Conf. Robot. Autom.*, 2016, pp. 1788–1793.

[15] ——, "Exponential stabilization of fully actuated planar bipedal robotic walking with global position tracking capabilities," *J. Dyn. Syst. Meas. Control*, vol. 140, no. 5, p. 051008, 2018.

[16] ——, "Time-dependent orbital stabilization of underactuated bipedal walking," in *Proc. American Contr. Conf.*, 2017, pp. 4858–4863.

[17] C. Chevallereau, J. W. Grizzle, and C.-L. Shih, "Asymptotically stable walking of a five-link underactuated 3-D bipedal robot," *IEEE Trans. Robot.*, vol. 25, no. 1, pp. 37–50, 2009.

[18] K. S. Fu, R. Gonzalez, and C. G. Lee, *Robotics: Control Sensing. Vis.* Tata McGraw-Hill Education, 1987.

[19] R. M. Murray, *A mathematical introduction to robotic manipulation*. CRC press, 2017.

[20] J.-J. E. Slotine and W. Li, "On the adaptive control of robot manipulators," *The international journal of robotics research*, vol. 6, no. 3, pp. 49–59, 1987.

[21] J. W. Grizzle, C. Chevallereau, R. W. Sinnet, and A. D. Ames, "Models, feedback control, and open problems of 3d bipedal robotic walking," *Automatica*, vol. 50, no. 8, pp. 1955–1988, 2014.

[22] B. Yao, "Adaptive robust control of nonlinear systems with application to control of mechanical systems," Ph.D. dissertation, University of California, Berkeley, 1996.

[23] M. Raibert, S. Tzafestas, and C. Tzafestas, "Comparative simulation study of three control techniques applied to a biped robot," in *Proceedings of IEEE Systems Man and Cybernetics Conference-SMC*, vol. 1. IEEE, 1993, pp. 494–502.

[24] P. A. Ioannou and J. Sun, *Robust adaptive control*. Courier Corporation, 2012.

[25] M. S. Branicky, "Multiple lyapunov functions and other analysis tools for switched and hybrid systems," *IEEE Transactions on automatic control*, vol. 43, no. 4, pp. 475–482, 1998.